

Supporting Information

Natural wood-derived free-standing films as efficient and stable separators for high-performance lithium ion batteries

Yunlong Yang,^a Ning Li,^a Tian Lv,^a Zilin Chen,^a Yanan Liu,^a Keyi Dong,^a Shaokui Cao,^b Tao Chen^{*a}

^aShanghai Key Lab of Chemical Assessment and Sustainability, School of Chemical Science and Engineering, Tongji University, Shanghai 200092, P. R. China. E-mail: tchen@tongji.edu.cn

^bSchool of Materials Science and Engineering, Zhengzhou University, Zhengzhou, 450001, China.

Materials and Methods

Materials

Pine wood, Basswood and Poplar wood were purchased from Qiaonan Building Materials Market, Tianshui City, Gansu Province. Sodium sulfite (>98%) and sodium hydroxide (>98%) were purchased from Sigma-Aldrich. Lithium electrode, LiFePO₄ and stainless steel electrode were purchased from Nanjing Lithing Corporation.

Modification of natural wood films

The wood films were fabricated by planing wood blocks along the growth direction of tree, and then, they were cut into strips or small pieces for further treatment. The obtained wood films were immersed in a mixed solution of sodium sulfite (0.4 mol L⁻¹) and sodium hydroxide (2.5 mol L⁻¹), followed by removing air in the pores of wood films for half an hour under a pressure of 200 Pa. The mixed solution and air-removed wood films were transferred into a stainless steel reactor and kept for 12 hours at 120 °C. The as-modified wood films were washed by using deionized water until the value of pH reached about 7.0. Then, the as-washed modified wood films were freeze-dried for 12 hours. Finally, the above modified wood films were transferred to a vacuum oven to remove residual traces of moisture before use.

Fabrication of electrode and lithium ion battery

The slurry was prepared by fully mixing LiFePO₄ (Sinopharm Chemical Reagent Co.), acetylene black (Shenzhen Kejingstar Co.) and poly(vinylidene difluoride) (PVDF) with the mass ratio of 8:1:1 in 1-methyl-2-pyrrolidinone (NMP). The positive electrode laminate was fabricated by casting the LiFePO₄ slurry on an aluminum foil, and followed by drying in a vacuum oven at 80 °C for 12 hours. The button batteries (2032-type coin) were assembled in an argon-filled glove box by using LiFePO₄ electrode laminates as positive electrode, Li metal as the counter electrode, 1 mol L⁻¹ LiPF₆ in ethylene carbonate (EC)/diethyl carbonate (DEC) (volume ratio of 1:1) as the electrolyte (Zhangjiagang Guotai-Huarong Co.), and the modified wood film (or Celgard 2325, PP) as separator, respectively.

Characterization

The morphologies of raw and modified wood films were characterized by field emission scanning electron microscopy (Hitachi S-4800). The thermal stability was determined by Thermogravimetric and Differential Scanning Calorimetry (NETZSCH STA 449F3). The X-ray diffraction patterns were conducted on a Bruker D6 Advance X-ray diffractometer with employing monochromated Cu-K α radiation at a scan rate of 5 °/min, the operating voltage and current were 40 kV and 40 mA, respectively. The mechanical performance of separators was measured by a mechanical test machine (HY-0350, Shanghai Hengyi Co. Ltd). FTIR spectra of wood-derived film were conducted by an IR spectrophotometer (Alpha, Bruker) with the range of wave numbers from 400 to 4000 cm⁻¹. The electrochemical performance of cells was measured on LAND CT2001A battery test system and electrochemical workstation (CHI 700E).

The porosities of the wood films were calculated by the equation:

$$\text{Porosity} = (m - m_0) / (\rho V) \quad (1)$$

where m_0 and m are the weight of the separators before and after soaking in n-butanol for enough time, respectively; ρ is the density of n-butanol; V is the volume of sample.

The ionic conductivity of the liquid electrolyte (1 M LiPF₆ in ethylene carbonate/diethyl carbonate) soaked in the wood-derived separator between two stainless-steels was measured via electrochemical impedance spectroscopy (EIS) in the frequency ranging from 1 to 10⁶ Hz and calculated by the following equation:

$$\sigma = L / (RS) \quad (2)$$

where σ is ionic conductivity (mS cm⁻¹), L (cm) and S (cm²) are the thickness and area of separator, respectively; R (Ω) is the resistance obtained from the EIS test.

The lithium ion transference number (t_{Li^+}) was characterized using a symmetric cell of

Li/wood-derived separator soaked with electrolyte)/Li by the Direct Current (DC) polarization and combined with EIS characterization.

The lithium ion transference number (t_{Li^+}) was calculated according to equation:

$$t_{\text{Li}^+} = I_s(\Delta V - R_0 I_0) / I_0(\Delta V - R_s I_s) \quad (3)$$

where I_0 and I_s are the initial and steady-state DC current, respectively; R_0 and R_s are the initial and steady state interfacial resistances, respectively; ΔV is the applied potential.

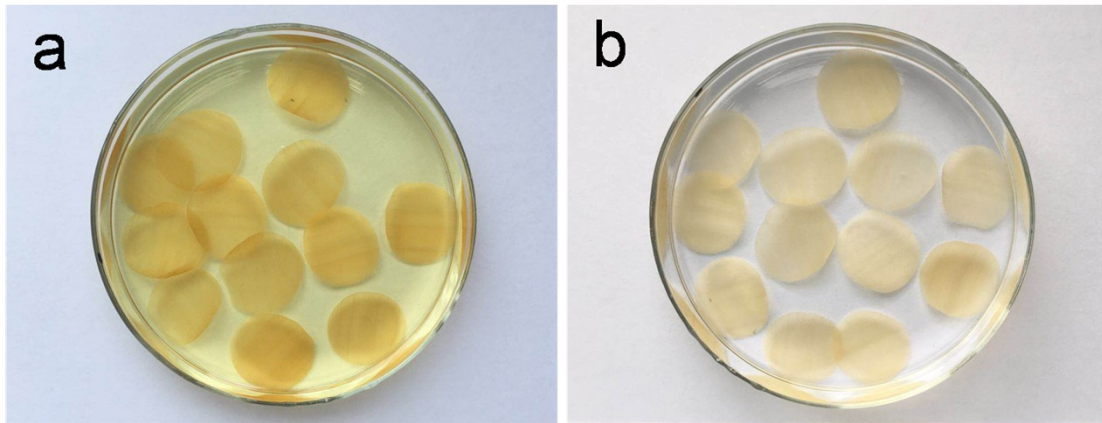


Fig. S1 Digital photographs of the as-modified natural wood films being washed in deionized water, (a) first-around washing, (b) washed to neutral.



Fig. S2 Flexibility of a piece of modified wood film.

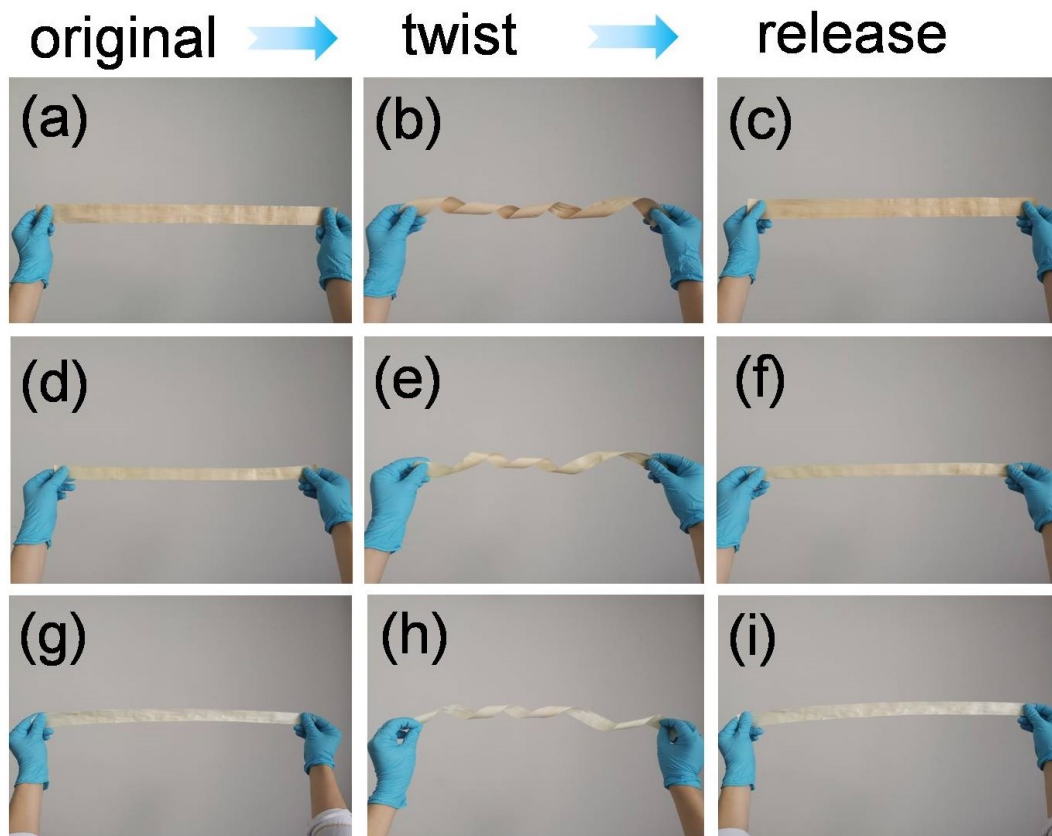


Fig. S3 Digital photographs of the modified natural wood film before and after twisting. (a-c) Modified film derived from wood 1. (d-f) Modified film derived from wood 2. (g-h) Modified film derived from wood 3.

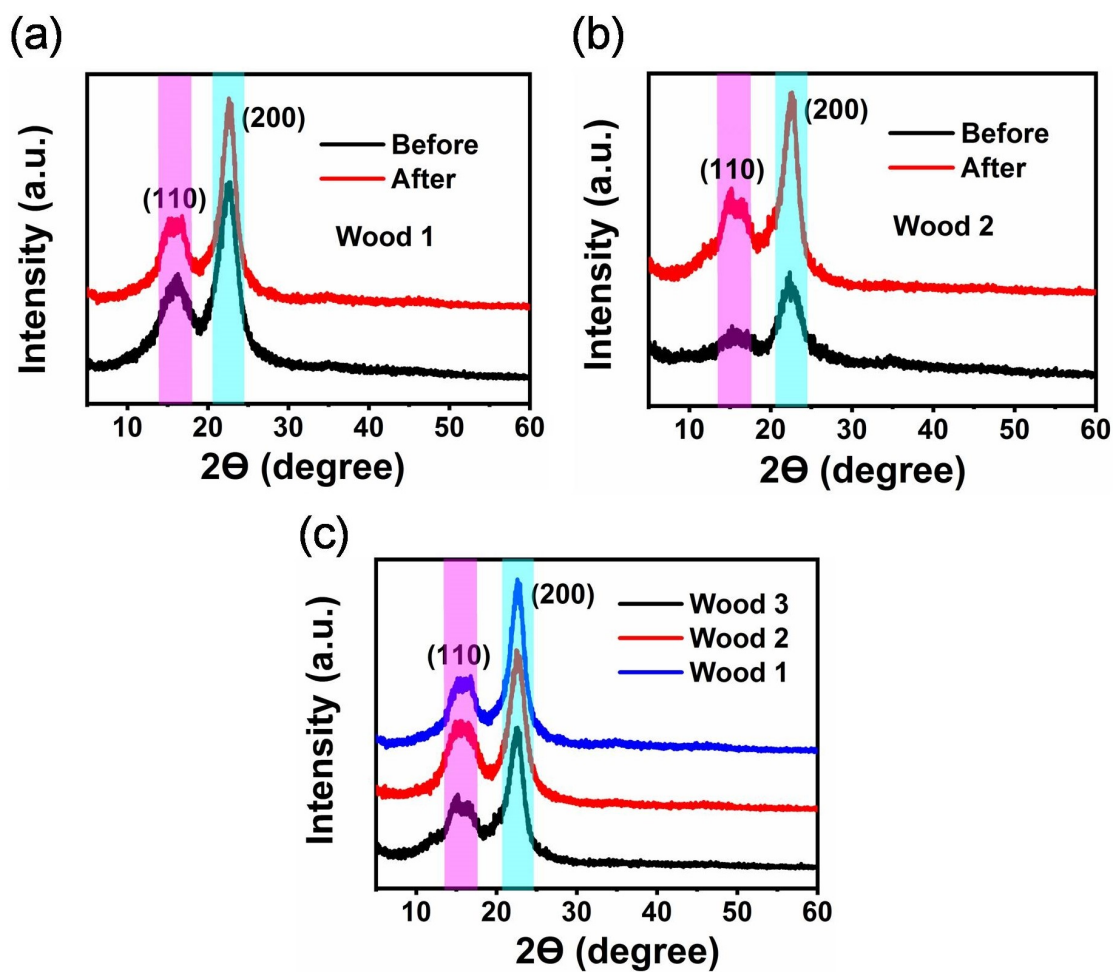


Fig. S4 X-ray diffraction patterns of different wood films before and after modification.

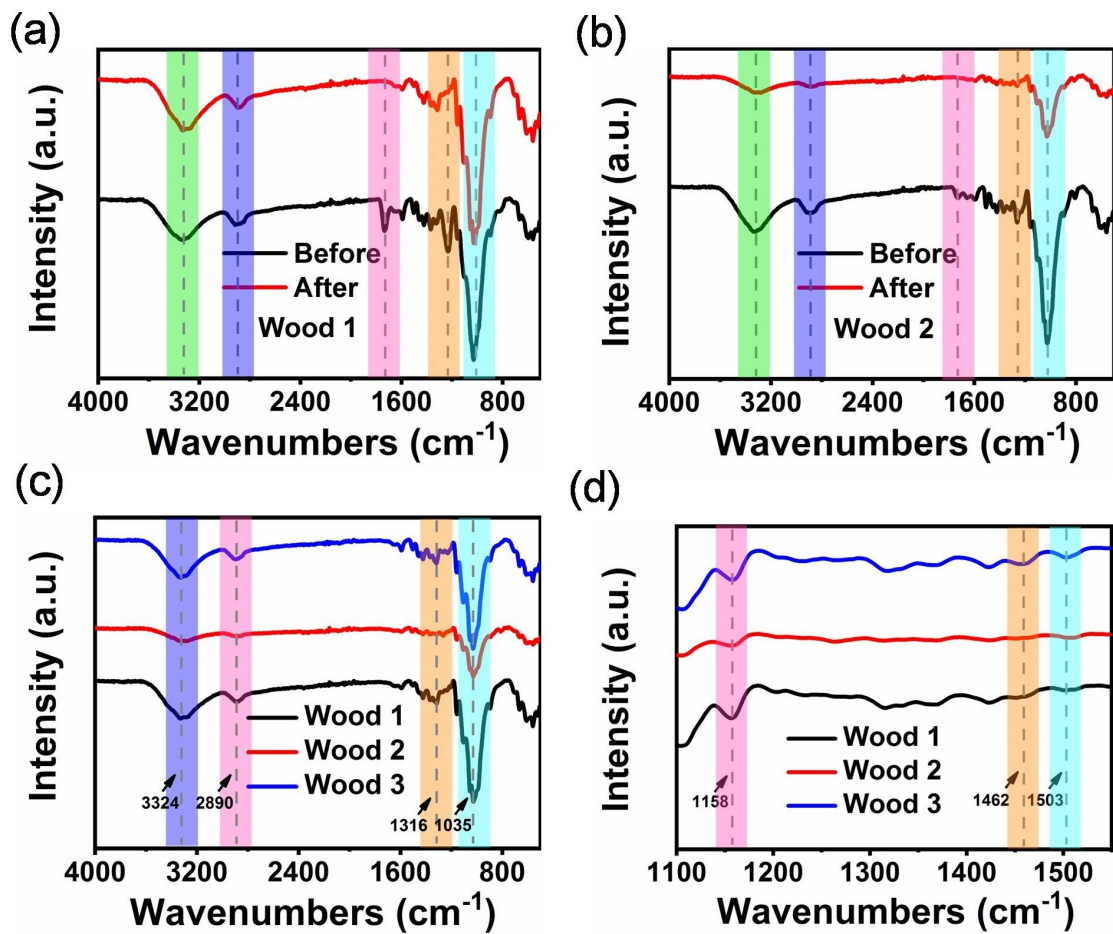


Fig. S5 FTIR spectra of different wood films before and after modification.

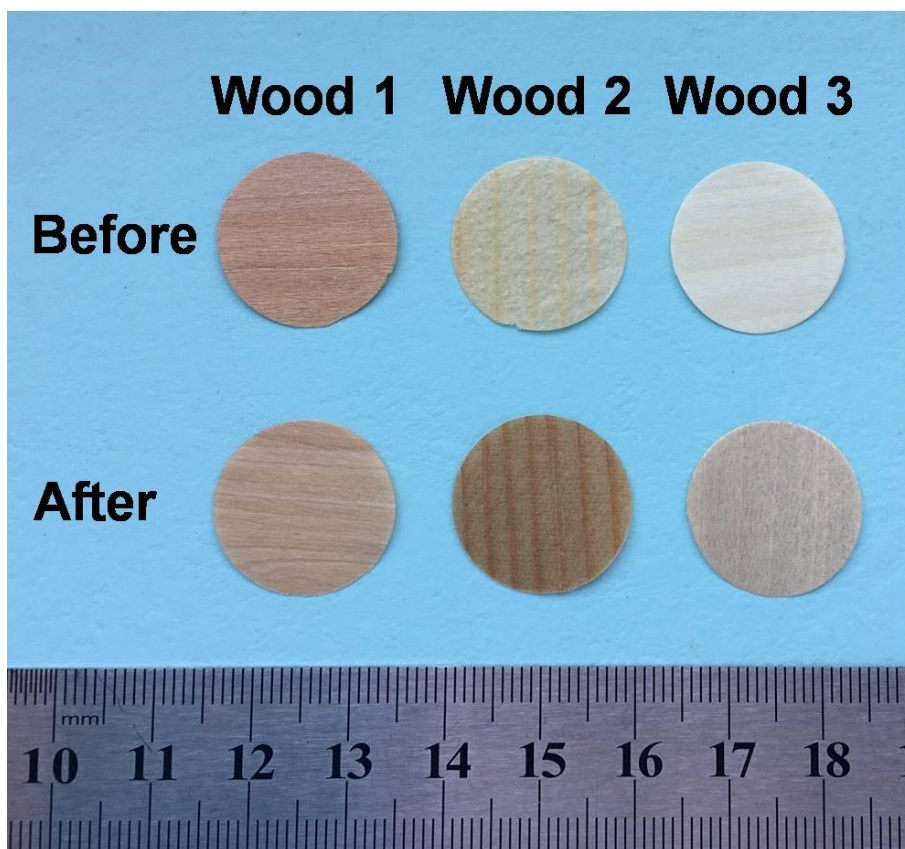


Fig. S6 Digital photographs of the different wood films before and after modification.

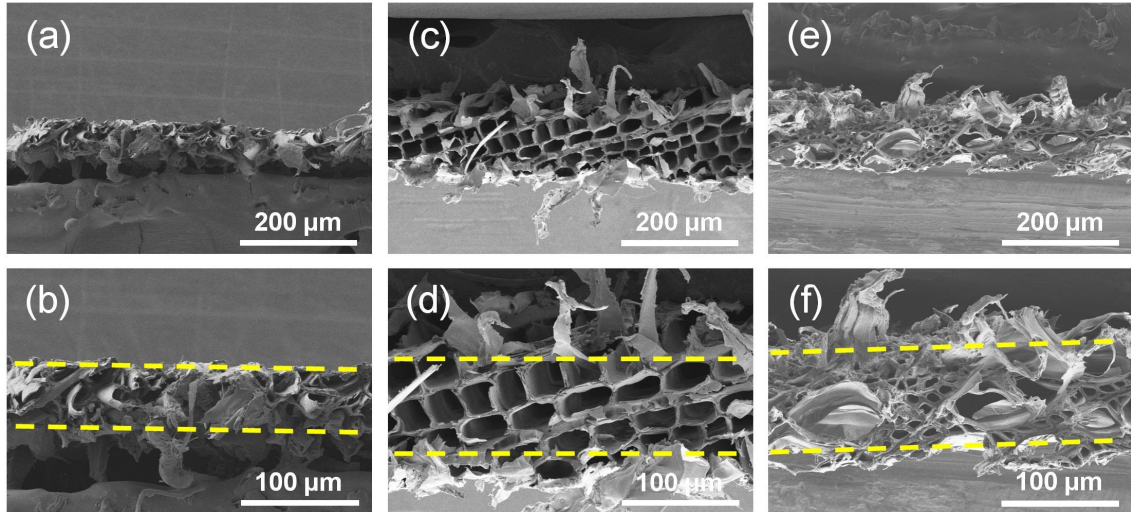


Fig. S7 SEM images of wood 1 (a and b), wood 2 (c and d) and wood 3 (e and f) without modification.

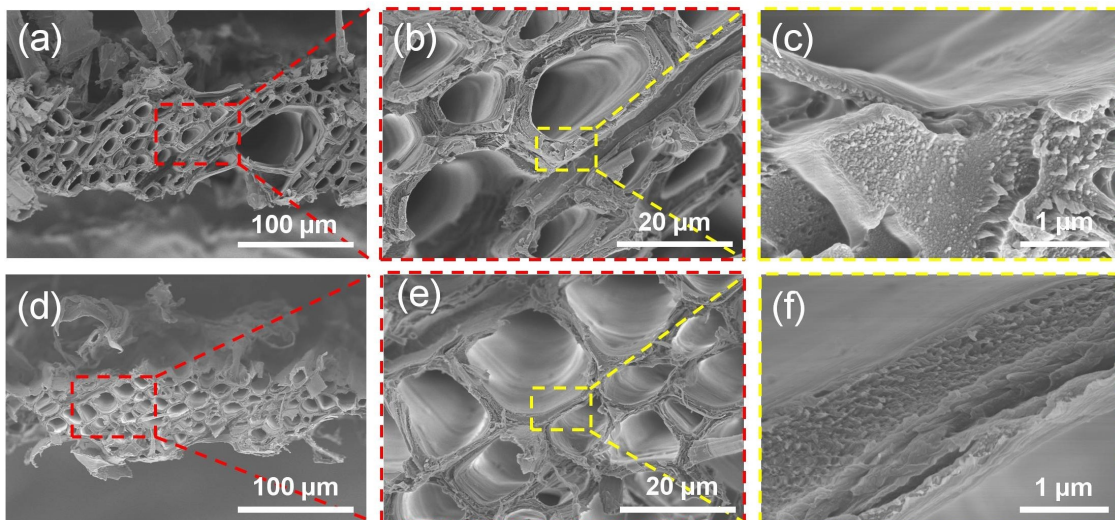


Fig. S8 SEM images of wood 3 before (a-c) and after (d-f) modification.

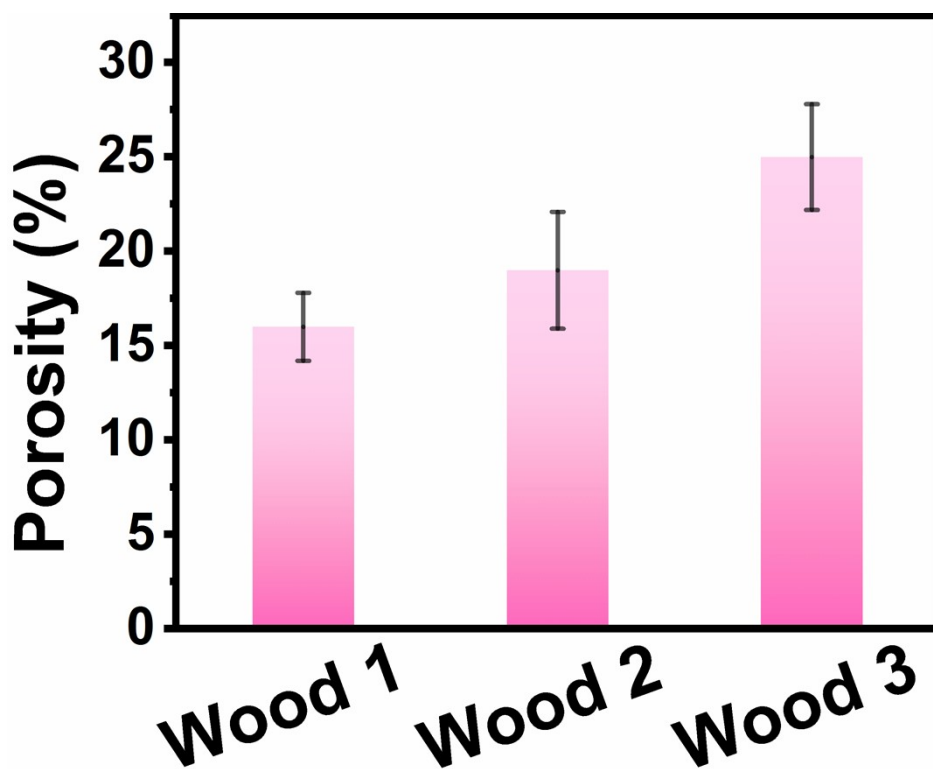


Fig. S9 Porosities of different modified wood films.

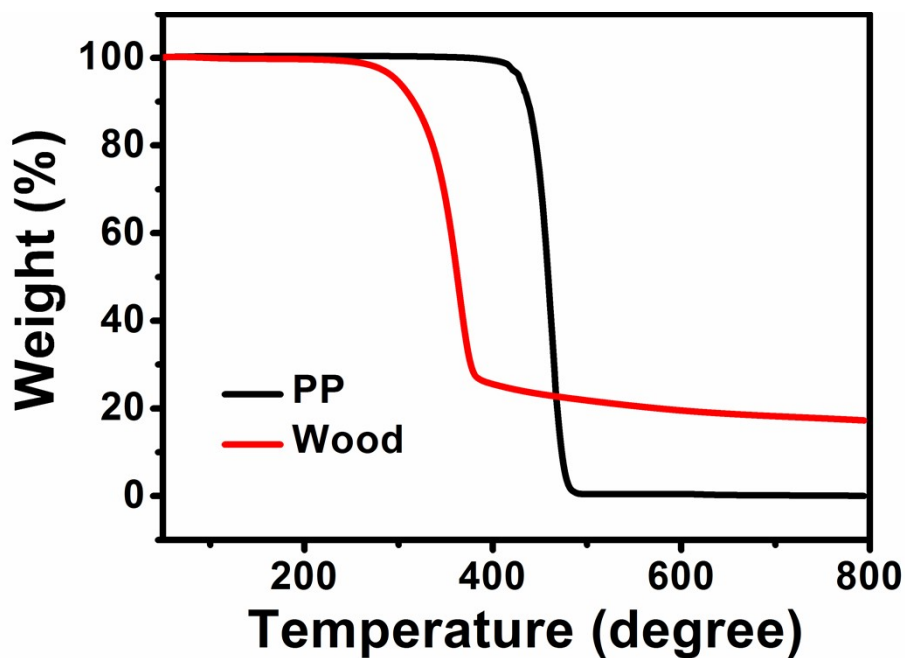


Fig. S10 TGA data of PP separator and wood 3-derived film.

Table S1. Comparison of our modified natural wood film with other reported biomass-derived separators. (I)

Materials	Stress MPa	Ionic conductivity mS cm⁻¹	Fabrication technique	Reference
Chitin nanofibers	77	0.066	Papermaking	Ref 1
WCDA/SiO ₂ /PE	110	0.32	Dip-coating	Ref 2
MC	20	0.2	Casting	Ref 3
MC/NWF	28	0.29	Casting	Ref 4
hydroxyethyl cellulose	10.2 8	0.18 0.4	Casting Electrospinning	Ref 5 Ref 6
PVDF-HFP/NCC				
CC	61	0.4	Filtration	Ref 7
Wood film	59	0.48	/	Our work

Table S2. Comparison of our modified natural wood film with other reported biomass-derived separators. (II)

Materials	Stress MPa	Li transfer number	Fabrication technique	Reference
methyl cellulose	20	0.29	Dip-coating	Ref 3
cellulose acetate/poly-L- lactic acid/ halloysite composite	3.0	0.3	Electrospinning	Ref 8
pristine cellulose nonwoven nonwoven	8	0.31	papermaking	Ref 9
fabric and methyl cellulose	28	0.34	Dip-coating	Ref 4
copolymer and cellulose	11.2	0.202	Dip-coating	Ref 10

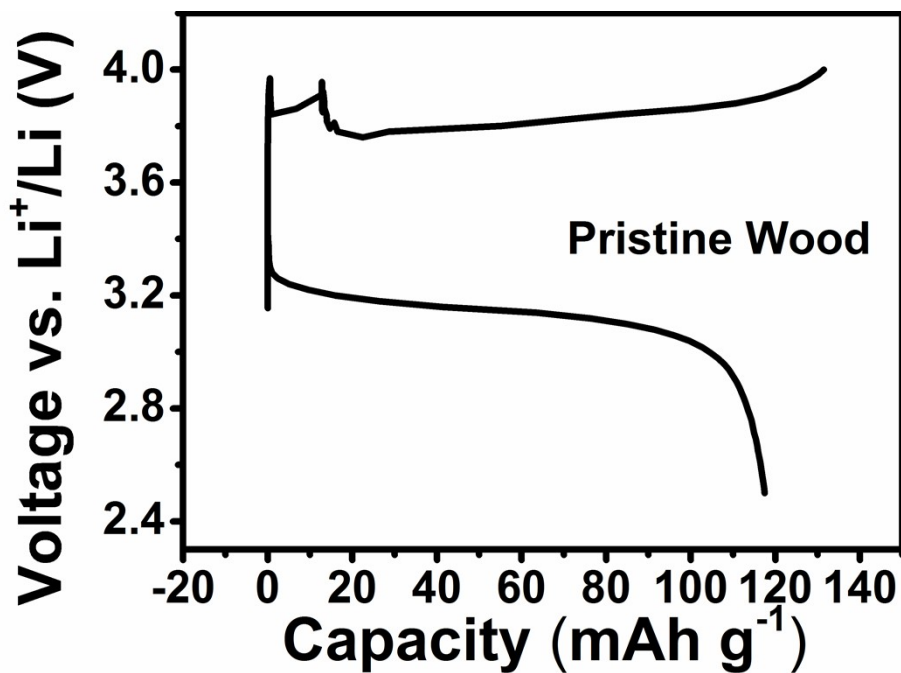


Fig. S11 Charge/discharge voltage profiles of the LiFePO₄/Li half-cells by using the separator of wood 3 without modification at 0.5 C (1 C = 170 mA g⁻¹).

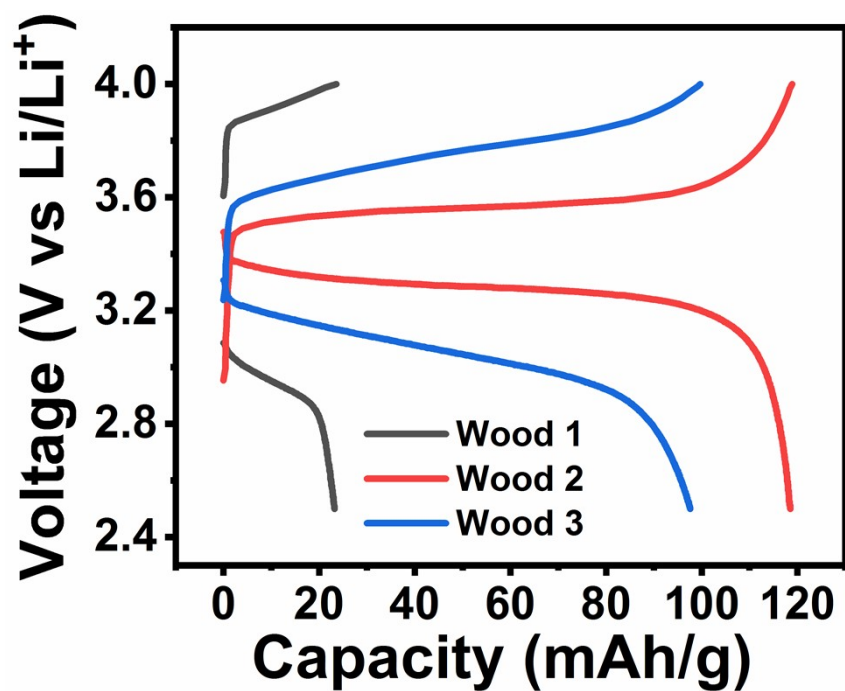


Fig. S12 Charge/discharge voltage profiles of the $\text{LiFePO}_4/\text{Li}$ half-cells with using the wood 3-derived separator dried in a common oven after hydrothermal treatment at 0.5 C ($1\text{ C} = 170\text{ mA g}^{-1}$).

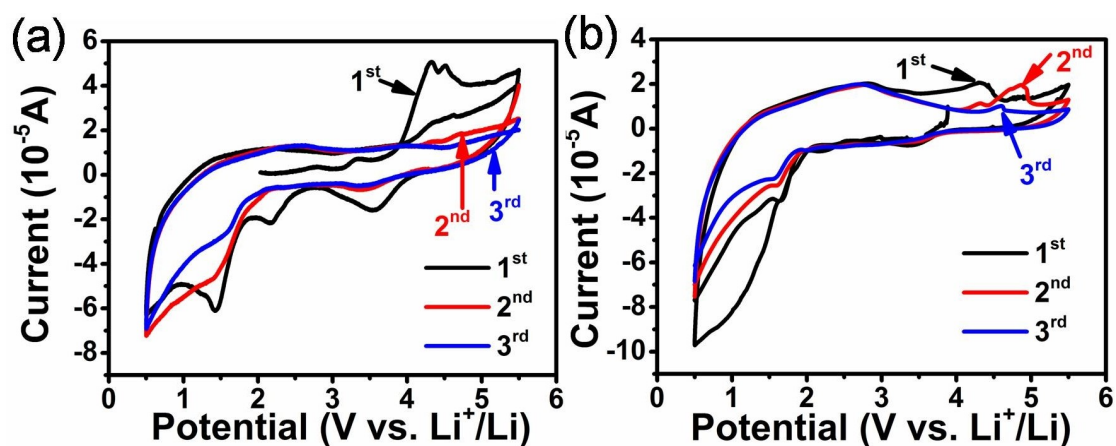


Fig. S13 Cyclic voltammograms of the $\text{LiFePO}_4/\text{Li}$ half-cells with using PP (a) and modified wood 3 film (b) as separator, respectively.

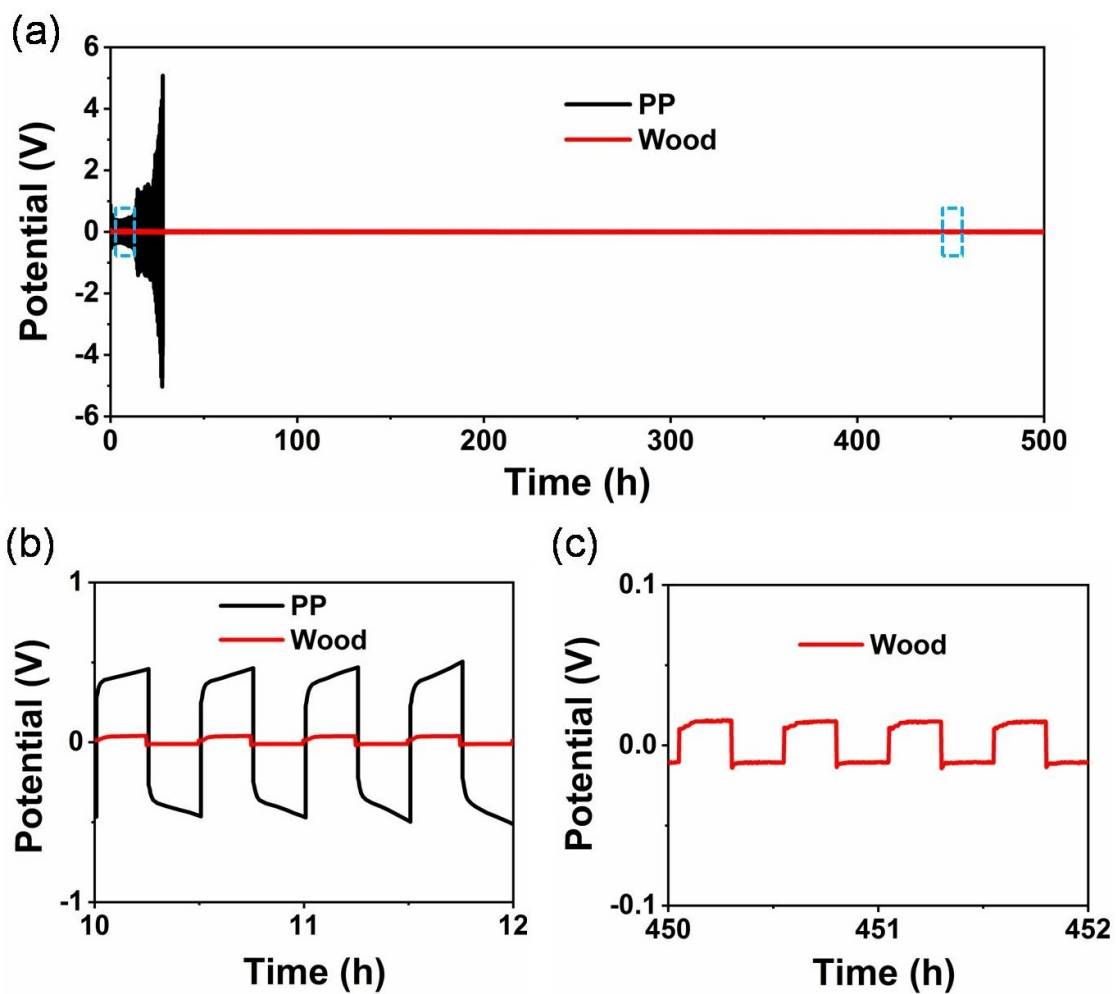


Fig. S14 (a) Voltage profiles of lithium symmetric cells with PP and wood 3-derived film as separators at a current density of 5 mA cm^{-2} for 500 hours (1000 cycles). (b) The detailed voltage profiles in the initial stage and (c) in the end of cycle test (1000 cycles).

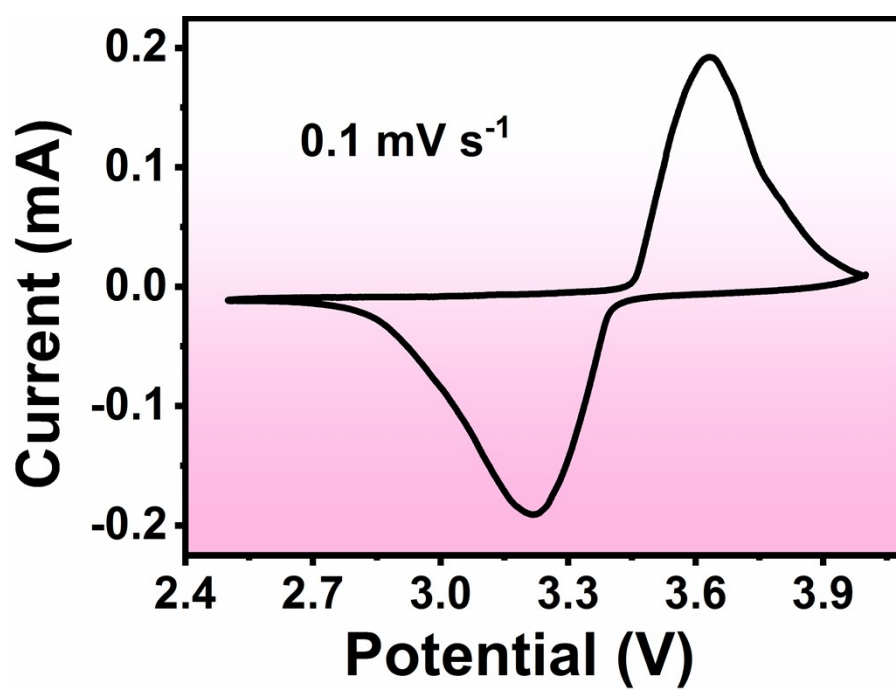


Fig. S15 Cyclic voltammogram of the LiFePO₄/Li half-cell with using the separator derived from wood 3 at a scan rate of 0.1 mV s⁻¹

Table S3. Comparison of electrochemical properties of our LiFePO₄/Li half-cells with that of devices by using other biomass separators reported previously.

Materials	Current density	Discharge capacity mAh g ⁻¹	Coulombic efficiency	cycles	Polarization voltage	References
methyl cellulose	0.2C	130	High 98%	55	3.2/3.6	Ref 4
Hydroxyethyl cellulose	0.2C	110	Low	60	3.12/3.63	Ref 5
Cladophora cellulose	0.2C	135	low	0.2 C	3.25/3.62	Ref 7
	1C	105		50		
Methyl cellulose	0.2C	130	high	0.2 C	3.15/3.7	Ref 3
	1C	60		40		
Carboxymethyl cellulose	0.1C	138	high	0.2 C	3.3/3.6	Ref 11
Egg shell membrane	0.2C	142				
	0.5C	128				
Egg shell membrane	1C	110	high	0.2 C	3.3/3.55	Ref 12
	0.1C	133				
	0.2C	75				
	0.5C	116				
Nanocrystalline cellulose	1C	60	high	0.2 C	3.3/3.55	Ref 6
	0.2C	85				
(NCC)-reinforced PVDF-HFP	0.5C	65	high	C	3.3/3.55	Ref 6
	1C	44				

Chitin	0.5C	131		0.5 C		
Nanofiber	1C	91	high	115	3.37/3.5	Ref 1
Membranes						
Wood	0.2C	138			3.375/3.47	
membrane	1C	117.7	high	80	3.25/3.58	Our work

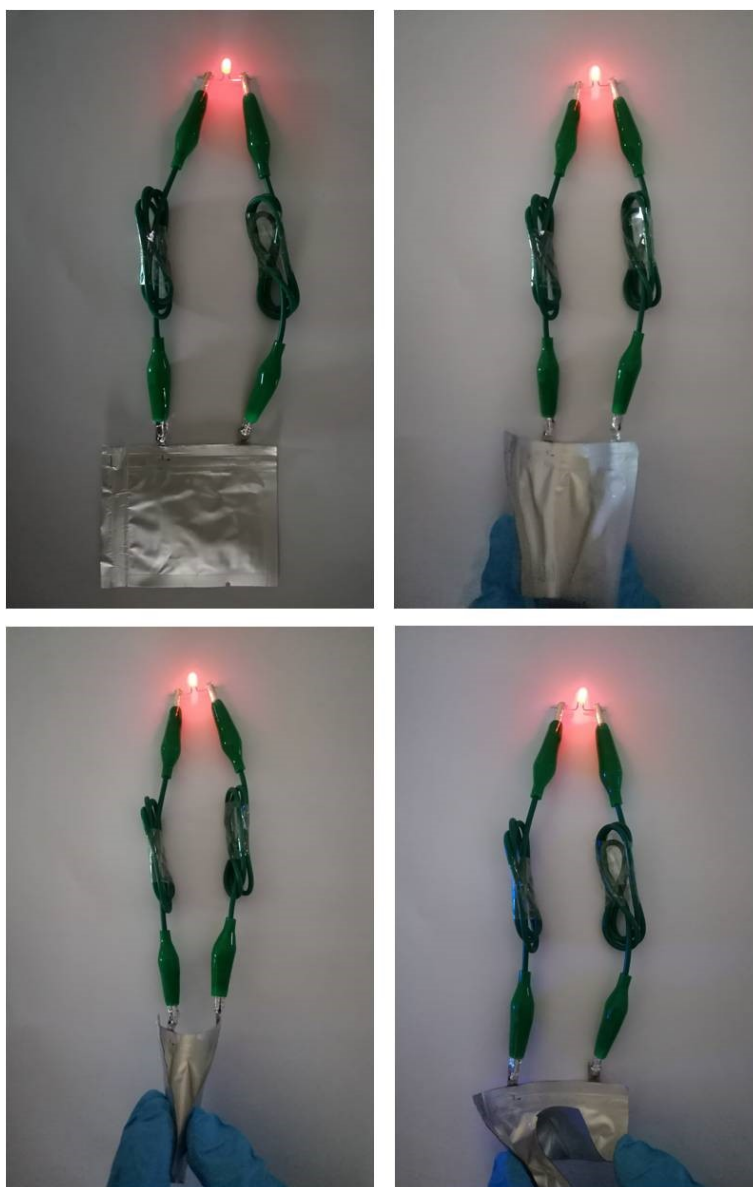


Fig. S16 The soft-packaging battery with using the natural wood-derived separator power a light-emitting diode under different bending states.

References

- [1] T. Zhang, B. Shen, H. Yao, T. Ma and S. Yu, *Nano Lett.*, 2017, 17, 4894-4901.
- [2] W. Chen, L. Shi, H. Zhou, J. Zhu, Z. Wang and S. Yuan. *ACS Sustain Chem. Eng.*, 2016, 4, 3794.
- [3] S. Xiao, F. Wang, Y. Yang, Z. Chang and Y. Wu, *RSC Adv.*, 2014, 4, 76-81.
- [4] Y. Wu, M. Li, X. Wang, Y. Wang and *RSC Adv.*, 2015, 5, 52382-52387.
- [5] X. Wang, W. Yang, Q. Chang and P. Holze, *J. Membr. Sci.*, 2015, 476, 112-118.
- [6] B. S. Lalia, Y. A. Samad and R. Hashaikeh, *J. Solid State Electrochem*, 2013, 17, 575-581.
- [7] R. Pan, O. Cheung, Z. Wang and P. Tammela. *J. Power Sources*, 2016, 321, 185-192.
- [8] M. Zhu, J. Lan, C. Tan, G. Sui and X. Yang, *J. Mater. Chem. A*, 2016, 4, 12136-12143.
- [9] G. Ding, B. Qin, Z. Liu, J. Zhang, B. Zhang, P. Hu, C. Zhang, G. Zhang, G. Xu, J. Yao and G. Cui, *J. Electrochem. Soc.*, 2015, 162, A834-A838.
- [10] J. Zhang, C. Ma, Q. Xia, J. Liu, Z. Ding and M. Xu, *J. Membr. Sci.*, 2016, 497, 259-269.
- [11] Y. Zhu, S. Xiao, M. Li, Z. Chang, F. Wang and J. Gao, *J. Power Sources*, 2015, 288, 368-375.
- [12] M. Raja, and A. M. Stephan, *RSC Adv.*, 2014, 4, 58546-58552.